



Noncanonical immune response to the inhibition of DNA methylation by Staufen1 via stabilization of endogenous retrovirus RNAs

Yongsuk Ku^{a,b,1}, Joo-Hwan Park^{c,d,1}, Ryeongun Cho^{a,b,1}, Yongki Lee^{a,b}, Hyoung-Min Park^e, MinA Kim^{a,b}, Kyunghoon Hur^{a,b}, Soo Young Byun^f, Jun Liu^{c,d}, Young-suk Lee^g, David Shum^f, Dong-Yeop Shin^{c,d}, Youngil Koh^{c,d}, Je-Yoel Cho^e, Sung-Soo Yoon^{c,d}, Junshik Hong^{c,d,2}, and Yoosik Kim^{a,b,2}

^aDepartment of Chemical and Biomolecular Engineering, Korea Advanced Institute of Science and Technology (KAIST), Daejeon 34141, Korea; ^bKAIST Institute for Health Science and Technology (KIHST), KAIST, Daejeon 34141, Korea; ^cDepartment of Internal Medicine, Seoul National University College of Medicine, Seoul National University Hospital, Seoul 03080, Korea; ^dCancer Research Institute, Seoul National University Hospital, Seoul 03080, Korea; ^eDepartment of Biochemistry, BK21 Plus and Research Institute for Veterinary Science, School of Veterinary Medicine, Seoul National University, Seoul 08826, Korea; ^fScreening Discovery Platform, Translation Research Division, Institut Pasteur Korea, Gyeonggi 13488, Korea; and ^gDepartment of Bio and Brain Engineering, KAIST, Daejeon 34141, Korea

Edited by Narry Kim, Seoul National University, Seoul, Republic of Korea, and approved February 22, 2021 (received for review August 3, 2020)

DNA-methyltransferase inhibitors (DNMTis), such as azacitidine and decitabine, are used clinically to treat myelodysplastic syndrome (MDS) and acute myeloid leukemia (AML). Decitabine activates the transcription of endogenous retroviruses (ERVs), which can induce immune response by acting as cellular double-stranded RNAs (dsRNAs). Yet, the posttranscriptional regulation of ERV dsRNAs remains uninvestigated. Here, we find that the viral mimicry and subsequent cell death in response to decitabine require the dsRNA-binding protein Staufen1 (Stau1). We show that Stau1 directly binds to ERV RNAs and stabilizes them in a genome-wide manner. Furthermore, Stau1-mediated stabilization requires a long noncoding RNA TINCR, which enhances the interaction between Stau1 and ERV RNAs. Analysis of a clinical patient cohort reveals that MDS and AML patients with lower Stau1 and TINCR expressions exhibit inferior treatment outcomes to DNMTi therapy. Overall, our study reveals the posttranscriptional regulatory mechanism of ERVs and identifies the Stau1-TINCR complex as a potential target for predicting the efficacy of DNMTis and other drugs that rely on dsRNAs.

DNA demethylation | double-stranded RNAs | noncoding RNA | RNA-binding protein | posttranscriptional regulation

Long double-stranded RNAs (dsRNAs) are duplex RNAs that can trigger an immune response by serving as an antigen for pattern recognition receptors (PRRs) (1). These RNAs are strongly associated with viral infection because they are produced as a replication byproduct of both DNA and RNA viruses, especially for positive-sense single-stranded RNA viruses (2, 3). The human genome encodes four different PRRs that can recognize long viral dsRNAs. They include melanoma differentiation-associated protein 5 (MDA5), protein kinase R (PKR), retinoic acid-inducible gene I (RIG-I), and toll-like receptor 3 (TLR3) (4, 5). Interestingly, these dsRNA sensors recognize the structural features of the target dsRNAs rather than their specific sequences. For example, PKR binds to dsRNAs longer than 33 base pairs (bp), which leads to dimerization and autophosphorylation of the protein (6–8). When phosphorylated, PKR becomes active and induces phosphorylation of a number of downstream substrates to suppress global translation and to initiate antiviral responses (9). This structure-based interaction may allow these immune response proteins to respond to a wide range of viruses with different genomic sequences.

Recent evidence suggests that the human genome contains numerous repeat elements that, when transcribed, can adopt a double-stranded secondary structure (10–12). Moreover, these cellular dsRNAs are also recognized by dsRNA immune sensors and activate them in uninfected cells. The most well-characterized cellular dsRNAs are from small-interspersed nuclear elements (SINEs), which are mostly Alus in primates. When transcribed with the host RNA, two Alu elements in the vicinity with the opposite

orientation can form intramolecular dsRNAs that are recognized by PKR and MDA5 as well as by other dsRNA-binding proteins (dsRBPs) such as adenosine deaminase acting on RNA (ADAR), which disrupts dsRNA structure by converting adenosine to inosine, and Staufen1 (Stau1), which affects the subcellular localization of Alu-containing mRNAs (13–18). In addition to Alus, recent studies have shown that RNAs from long-interspersed nuclear elements (LINEs), endogenous retroviruses (ERVs), and even mitochondrial RNAs (mtRNAs) can act as cellular dsRNAs to regulate antiviral signaling under physiological conditions (19–22). More importantly, these cellular dsRNAs are strongly associated with human diseases where the misactivation of PKR and MDA5 is reported (23). For example, mutations in ADAR and subsequent immune response by unedited Alu dsRNAs are associated with Aicardi-Goutières syndrome while patients with mutations in PNPase, which degrades mtRNAs, show strong interferon signatures (14, 21, 24).

Significance

Understanding the working mechanism of a chemotherapy drug is a critical step toward achieving the patient-specific treatment strategy. Decitabine is an FDA-approved drug being used to treat myelodysplastic syndrome (MDS) and acute myeloid leukemia (AML). Here, we employed an image-based screening platform to investigate the downstream factors of decitabine. We find that an RNA-binding protein Staufen1 (Stau1) is required for decitabine-mediated cancer cell death. We show that Stau1 stabilizes endogenous retrovirus RNAs induced by decitabine and transforms cells into the viral mimicry state. Indeed, MDS/AML patients with lower Stau1 expression show inferior response to decitabine. Our study unravels stabilization of key regulatory RNAs by Stau1 and suggests its potential use to predict decitabine-mediated therapy outcomes in clinics.

Author contributions: Y. Ku, J.-H.P., R.C., M.A.K., D.S., J.H., and Y. Kim designed research; Y. Ku, J.-H.P., R.C., Y.L., M.A.K., K.H., S.Y.B., and J.L. performed research; Y.-s.L. contributed new reagents/analytic tools; Y. Ku, J.-H.P., R.C., Y.L., H.-M.P., M.A.K., K.H., Y.-s.L., D.S., D.-Y.S., Y. Koh, J.-Y.C., S.-S.Y., J.H., and Y. Kim analyzed data; and Y. Ku, J.-H.P., R.C., Y.-s.L., J.H., and Y. Kim wrote the paper.

The authors declare no competing interest.

This article is a PNAS Direct Submission.

Published under the PNAS license.

¹Y. Ku, J.-H.P., and R.C. contributed equally to this work.

²To whom correspondence may be addressed. Email: hongjblood@snu.ac.kr or ysoosik@kaist.ac.kr.

This article contains supporting information online at <https://www.pnas.org/lookup/suppl/doi:10.1073/pnas.2016289118/-DCSupplemental>.

Published March 24, 2021.

Since cellular dsRNAs can activate immune response proteins, the expression of these RNAs is usually silenced through epigenetic regulation. Consequently, when cancer cells were treated with DNA-methyltransferase inhibitors (DNMTis), decitabine and azacitidine, the expression of ERV RNAs was induced, which resulted in MDA5 activation and subsequent cell death (19, 20). Recent studies have shown that in addition to MDA5, OAS-RNase L also mediates the downstream effect of ERV induction (25). Moreover, vitamin C enhances the effect of DNMTis by increasing the expression of ERV RNAs (26). This kind of induction of interferon response is now regarded as one of the most important mechanisms of action of DNMTis. Yet, our understanding of ERV RNAs at the posttranscriptional level is still limited. Considering that many dsRBPs, such as ADAR and Stau1, share a similar target pool as that of MDA5 and PKR, these proteins may also bind to ERV RNAs and affect response to DNMTi therapy. Considering that there still is no widely accepted predictive or prognostic biomarker of DNMTis, investigation on the regulatory factors of ERV RNAs may lead to the discovery of novel markers to predict the responsiveness or prognosis to DNMTi therapy.

In this study, we employ an image-based RNA interference (RNAi) screening platform to identify dsRBPs that affect immune response by cellular dsRNAs. We analyze the effect of the knockdown of eight dsRBPs individually and in pairs to examine their synergistic regulation in response to DNMTis. We find that Stau1 is required to transform cells to the viral mimicry state and induce cell death when decitabine is treated. We further show that Stau1 directly binds to ERV RNAs and regulates their stability and/or subcellular localization. Using formaldehyde-mediated cross-linking precipitation and sequencing (fCLIP-seq), we find that Stau1-mediated stabilization of ERV RNAs and the subsequent immune response occur in a genome-wide manner and even without decitabine treatment. Furthermore, we show that Stau1 stabilizes ERV RNAs through a cofactor TINCR long noncoding RNA, which forms a complex with Stau1 and enhances the interaction between Stau1 and ERV RNAs. Lastly, we provide a clinical significance of our findings by analyzing a clinical cohort of high-risk myelodysplastic syndrome (MDS) or acute myeloid leukemia (AML) patients who received frontline DNMTi therapy. We find that patients with lower Stau1 and TINCR expressions showed significantly inferior treatment outcomes, both in progression-free survival (PFS) and overall survival (OS). Collectively, our study establishes the functional role of Stau1 in its stabilization of cellular dsRNAs and its potential use to predict the outcomes of DNMTi therapy in clinics.

Result

Multiple dsRBPs Affect Response to Low-Dose Exposure to Decitabine.

Transient low-dose treatment of decitabine to colorectal cancer cells results in cell death via viral mimicry (19, 20). Here, we applied a similar experimental system where we treated HCT116 cells with 0.5 μ M of decitabine for 24 h and cultured cells in fresh media for 4 d. Consistent with previous studies, we also observed a delay in doubling time starting 2 d after the treatment and significant cell death by the fifth day (Fig. 1A). We extracted total RNAs and confirmed that many ERV RNAs were strongly induced, which resulted in the increased expression of several interferon-stimulated genes (ISGs) (Fig. 1B and C). Indeed, in MDA5-deficient cells, the induction of ISGs was nearly abrogated, which resulted in increased cell proliferation (Fig. 1C and D). However, the degree of the increase in cell proliferation in MDA5-deficient cells was too small, indicating that there may exist other factors that regulate response to decitabine.

One strong candidate was PKR, another member of the dsRNA-recognizing innate immune response system. Using PKR fCLIP-seq, we have previously shown that PKR can bind to ERV RNAs (22). Considering that PKR only requires dsRNAs longer than 33 bp to become activated (27), the PKR signaling system is likely to be regulated by ERV RNAs during decitabine

treatment. Indeed, we found that phosphorylated PKR (pPKR) as well as phosphorylation of eIF2 α , the primary downstream substrate of PKR, were increased 5 d after decitabine treatment (SI Appendix, Fig. S1A–C). Moreover, PKR-deficient cells showed significant rescue in cell viability, even stronger than that of MDA5 knockdown (SI Appendix, Fig. S1D–F). Therefore, both PKR and MDA5 are involved in response to decitabine.

In addition to PKR, the human genome encodes multiple dsRBPs that share similar dsRNA-binding domains (dsRBDs). These dsRBDs can only recognize the structural features of the target dsRNAs (28). Indeed, previous high-throughput studies have shown that dsRBPs, such as ADAR, Stau1, DEXH-Box Helicase 9 (DHX9), and PKR, all bind and regulate or are regulated by Alu dsRNAs (18, 22, 29, 30). Considering that PKR could bind to ERV RNAs and that the down-regulation of PKR significantly rescued cell death by decitabine treatment, many other dsRBPs would participate in response to ERV induction by decitabine. Moreover, these dsRBPs may work together or against each other in response to increased ERV RNA expressions.

To investigate and identify dsRBP factors that regulate decitabine-mediated cell death, we employed an image-based high-throughput screening platform. We first performed an initial screening of 14 dsRBPs and chose 8 based on their function and ability to mediate the downstream effect of decitabine. We used the same experimental set up used for our analysis of MDA5 and PKR, where we transfected cells with a siRNA targeting a specific dsRBP twice over a 6-d period to ensure suppression of the target protein expression throughout the experiment (Fig. 1E). We found that Stau1 knockdown resulted in the strongest degree of rescue in cell viability while no dsRBP alone could enhance the apoptotic effect of decitabine (Fig. 1F). Consistent with our earlier experiments, MDA5 knockdown only had a moderate effect while PKR knockdown had an intermediate effect; it was stronger than MDA5, but weaker than that of Stau1. When we performed the same screening assay using a combinatorial knockdown of two dsRBPs, we could clearly observe synergistic effects. Most of the dsRBPs worked together with Stau1 in that when Stau1 and another dsRBP were both knocked down, a significant rescue was observed (Fig. 1G). Interestingly, the combinatorial knockdown of DHX9 and protein activator of PKR (PACT) enhanced the effect of decitabine. In this context, DHX9 and PACT were working together to sensitize cells to decitabine. Antagonistic effects were also observed where the knockdown of PACT or DHX9 canceled the rescue effect of Stau1 knockdown (Fig. 1G).

Stau1 Regulates the Expression and Localization of ERV RNAs.

We focused on Stau1-mediated regulation and asked how Stau1 affects the response to decitabine, especially with respect to the posttranscriptional regulation of ERV RNAs. We designed multiple siRNAs that target either CDS or 3' UTR of the *Stau1* mRNA and confirmed their knockdown efficiencies through Western blotting (Fig. 2A). We then confirmed that Stau1 knockdown almost completely rescued cell death by decitabine treatment, which was consistent with our image-based screening result (Fig. 2B). More importantly, we showed that Stau1 knockdown alone without decitabine did not affect the cell proliferation rate, indicating that the observed effect was not through Stau1 knockdown affecting the cell doubling time independent of decitabine (Fig. 2B). To investigate the mechanism, we first asked whether Stau1 could directly interact with ERV RNAs. We performed Stau1 fCLIP followed by qPCR analysis and showed that Stau1 strongly interacted with several ERV RNAs when decitabine was treated (Fig. 2C). Next, we examined the expression of ERV RNAs in Stau1-deficient cells and found that the level of most ERV RNAs was significantly decreased (Fig. 2D). This result was unexpected because Stau1 was known to destabilize dsRNAs by triggering Staufen-mediated

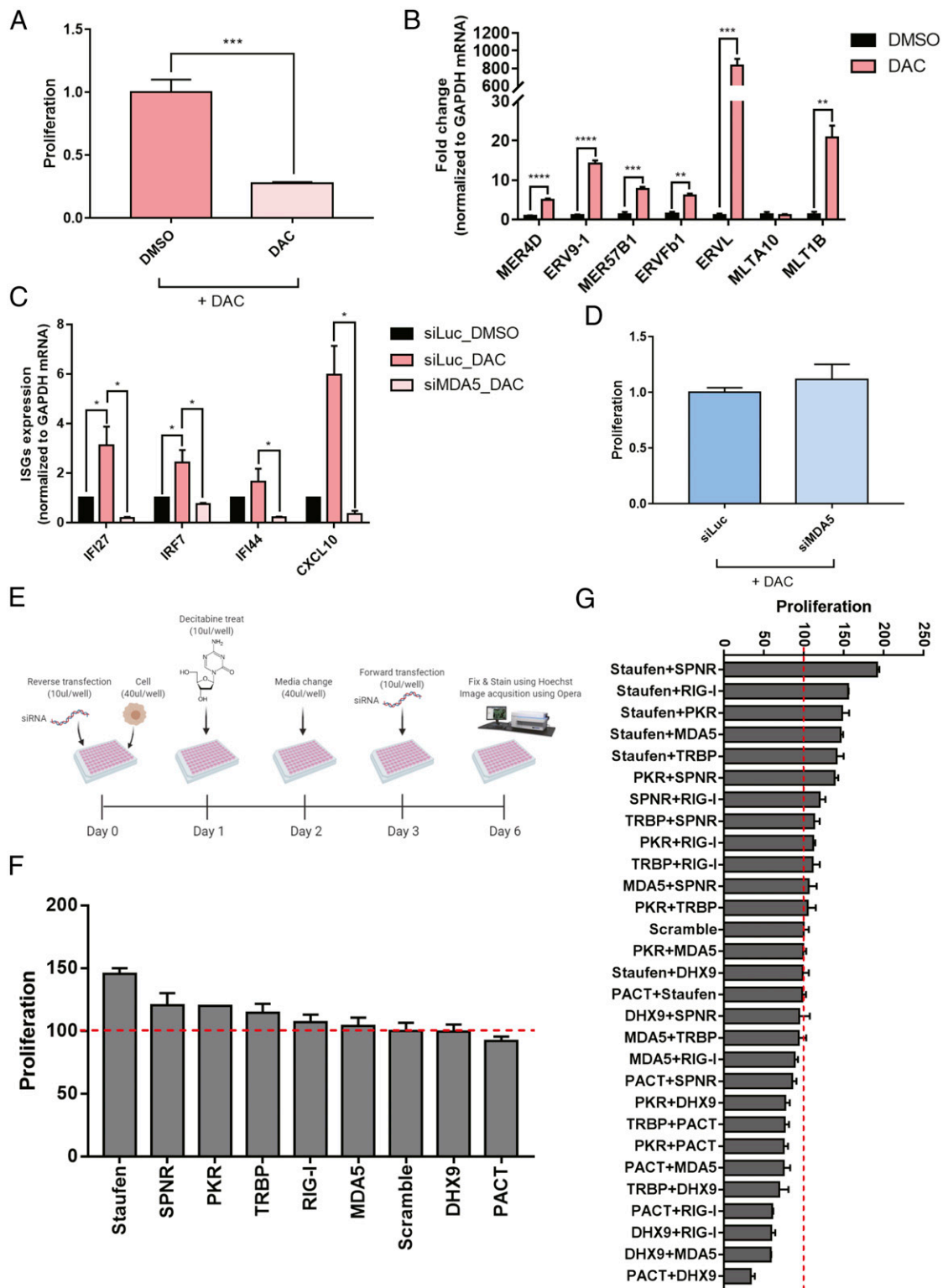


Fig. 1. Several dsRBPs affect cell death by transient low-dose exposure to decitabine. (A) Transient low-dose exposure to decitabine for 5 d resulted in a significant decrease in proliferation measured by sulforhodamine B (SRB) assay. (B) The induction of several ERV RNAs by decitabine treatment was confirmed using RT-qPCR. (C) Moreover, increased ERV RNA levels led to MDA5-dependent induction of ISGs. (D) The knockdown of MDA5 partially rescued cell death by decitabine. (E) A schematic of the image-based dsRBP screening employed in this study (created with [BioRender.com](https://www.biorender.com)). (F and G) Cell proliferation results of image-based RNAi screening when dsRBPs were knocked down individually (F) or in pairs (G). In all experiments, an average of three biological replicates are shown with error bars denoting SEM. A Student's *t* test was performed for statistical analysis. **P* value <0.05, ***P* value <0.01, ****P* value <0.001, *****P* value <0.0001.

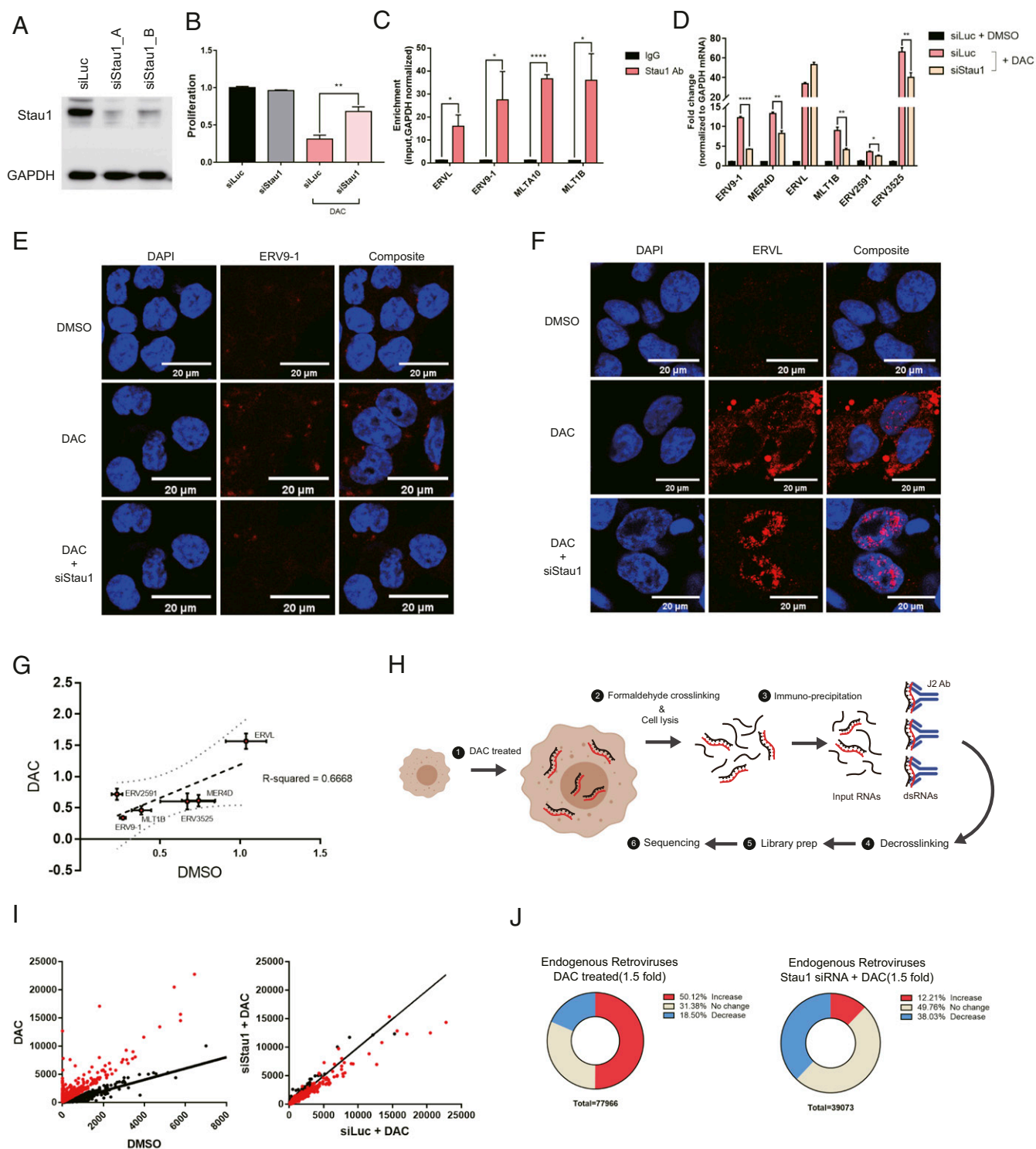


Fig. 2. Stau1 interacts with ERVs and regulates their expression and localization. (A) Western blot result to confirm the knockdown efficiency of siRNAs used in this study. siStau1_A targets the 3' UTR of Stau1 mRNA while siStau1_B targets the coding region of the mRNA. We present the data using siStau1_A for the rest of the study, but siStau1_B also yielded similar results. (B) The knockdown of Stau1 significantly rescued cell death from decitabine treatment. $n = 3$ and error bars denote SEM. (C) Direct interaction between Stau1 and ERV RNAs was confirmed using RNA immunoprecipitation (RNA-IP) after formaldehyde cross-linking. $n = 3$ and error bars denote SEM. Enrichment relative to that of GAPDH mRNA is shown. (D) Knockdown of Stau1 resulted in decreased expression of most ERV RNAs examined. $n = 3$ and error bars denote SEM. (E and F) RNA FISH of ERV9-1 (E) and ERVL (F) revealed that Stau1 could affect the expression and subcellular localization of ERV RNAs. (G) Stau1 knockdown also affected the basal expression of ERV RNAs without decitabine. Fractional change of ERV RNA expression levels assessed by RT-qPCR for DMSO control and decitabine-treated samples is shown. The two conditions show a good positive correlation with $R^2 = 0.6668$. (H) A schematic for the J2 fCLIP dsRNA-seq process. (Created with [BioRender.com](https://www.biorender.com).) (I) Distribution of ERV RNA expression in the J2 dsRNA-seq result. Each dot represents sequencing reads mapped to a specific ERV locus. Red dots represent ERV loci with at least a 1.5-fold increase in expression by decitabine. (J) Pie chart of percent of ERV loci with a change in expression by decitabine and in Stau1 knockdown cells. * P value < 0.05 , ** P value < 0.01 , *** P value < 0.001 , **** P value < 0.0001 .

decay (SMD) (31). On the contrary, our results show that, in the case of ERV RNAs, Stau1 stabilizes the dsRNA transcript.

For ERV9-1, we designed complementary RNA probes and performed fluorescent in situ hybridization (FISH) to visualize the RNA expression pattern. While the control dimethyl sulfoxide (DMSO)-treated cells did not show any ERV9-1 RNA-FISH signal, decitabine-treated cells showed strong signals throughout the cytosol, indicating the induction of ERV9-1 RNAs (Fig. 2E). However, in Stau1 knockdown cells, the ERV9-1 was almost completely eliminated (Fig. 2E). Furthermore, we also examined ERVL RNA because it was the only ERV type whose expression was not decreased in Stau1-deficient cells. Surprisingly, we found that when Stau1 was knocked down, the subcellular localization of ERVL RNA was altered from cytosolic to mostly nuclear (Fig. 2F). In this context, Stau1 may be important in the cytosolic export of ERVL RNA, similar to its role in the regulation of dsRNAs formed by inverted Alu repeats (13). Lastly, we examined whether Stau1 could affect the basal expression of ERV RNAs without decitabine induction. We found that for most ERV RNAs examined, Stau1 knockdown decreased their basal expression levels as well. When we plotted the percent change of ERV RNAs in control versus decitabine-treated cells, the two conditions show a good positive correlation, indicating that Stau1 might be a general regulator of ERV dsRNA expression regardless of decitabine treatment (Fig. 2G).

Encouraged by these results, we performed a genome-wide analysis to examine and identify ERV elements that were regulated by Stau1. The human genome encodes about 98,000 ERV loci, but it is unclear the percent of these ERV loci potentially induced by decitabine and the fraction of these ERV RNAs that were also regulated by Stau1. First, we analyzed ERV RNAs using total RNA-seq. However, the sequencing reads mapped to the ERV elements were too few that we could not obtain statistically meaningful results for most ERV loci. Instead, we enriched dsRNAs through FCLIP using J2 dsRNA antibody and analyzed immunoprecipitated dsRNAs by high-throughput sequencing (Fig. 2H). Through this approach, we were able to map a significant number of sequencing reads to about 78,000 ERV loci. Sequencing read accumulation and change on an exemplary ERV element (ERV1_LTR1_3525) are shown in *SI Appendix, Fig. S24*. Structural prediction using RNAfold clearly revealed that this ERV element was likely to generate the dsRNA structure when transcribed (*SI Appendix, Fig. S2B*). Among the 78,000 identified ERV elements, we found that about 50% (~39,000) of ERV elements showed at least a 1.5-fold increase in RNA expression (Fig. 2I and J). Out of these ERV elements, about 40% showed at least a 1.5-fold decrease in expression when Stau1 was knocked down. Of note, when we analyzed our sequencing data for other retrotransposon elements that could generate dsRNAs, such as SINE and LINE, we found that SINE RNAs were also induced by decitabine to such a degree that the proportion of ERV was decreased in decitabine-treated cells (*SI Appendix, Fig. S2C*). This is consistent with a recent report that the major source of immunogenic dsRNAs induced by DNMT1 is Alu elements (32). Interestingly, the proportion of sequencing reads occupied by SINE/Alu was decreased when Stau1 was knocked down, indicating that Alu RNAs might also be regulated by Stau1. We confirmed the decreased expression of a number of Alu RNAs in Stau1-deficient cells (*SI Appendix, Fig. S2D*). Although the current study is focused on ERV RNAs, our data indicate that decitabine may regulate other cellular dsRNAs, particularly those from retrotransposable elements and that Stau1 also affects the expression level of cellular dsRNAs in addition to ERVs.

Restoring Stau1 Can Rescue the ERV Expression. As our analysis was based on RNAi-mediated gene knockdown, we further complemented the data by generating Stau1 knockout (KO) HCT116 cells. We designed a sgRNA targeting the exon 7 of Stau1 locus

and successfully generated a frameshift mutant. The Western blotting analysis showed the complete elimination of the band corresponding to Stau1 protein (Fig. 3A). Of note, we were able to detect a weak band slightly smaller than the size of wild-type Stau1. Using a siRNA, we confirmed that this residual band was not from truncated Stau1, but likely a background (Fig. 3A). In Stau1 KO cells, we examined the induction of ERV RNAs upon transient exposure to low-dose decitabine. We found that the magnitude of ERV induction was significantly reduced in the KO cells (Fig. 3B).

We then performed rescue experiments by overexpressing Stau1 in the KO cells. We found that for all of the ERVs examined, overexpressing Stau1 resulted in increased expression (Fig. 3C). For ERV9-1, increased RNA expression was further confirmed via RNA-FISH. For this analysis, we identified Stau1-expressing cells using the Flag tag on the exogenous Stau1 protein (green) and compared the red fluorescent signal intensities from ERV9-1 RNAs with those from the cells that do not express Stau1 protein. We found that the Stau1-expressing cells showed significantly higher red fluorescent intensities, indicating the higher expression of ERV9-1 RNAs (Fig. 3D). We also utilized the KO cells to further examine the mechanism of Stau1-mediated ERV regulation. We treated cells with actinomycin D (ActD) to shut down the transcription and analyzed the stability of ERV RNAs over time. The ERV RNA expression was normalized to that of the U6 small nucleolar RNA, which is transcribed by polymerase III and is not affected by ActD. Compared to the parental cells, the KO cells showed decreased expression of ERV RNAs, indicating faster degradation of the RNAs (Fig. 3E). Therefore, Stau1 affects the ERV RNA expression by directly binding and stabilizing the transcript.

Stau1 Affects the Immune Response by Decitabine. Next, we asked whether Stau1 also affects the viral mimicry state induced by decitabine. First, we examined the effect of Stau1 knockdown on the activation status of PKR and its downstream signaling. Since ERV and other dsRNAs act as PKR activators, Stau1 knockdown should decrease the phosphorylation of PKR and its downstream signaling even when cells were treated with decitabine. Using immunocytochemistry, we found that, in Stau1-deficient cells, both pPKR and pEIF2 α signals were decreased dramatically (*SI Appendix, Fig. S3*). The signal for the total PKR and eIF2 α remained unchanged, indicating that Stau1 affects the activation status of PKR signaling by stabilizing PKR-activating dsRNAs such as ERVs.

We then investigated the effect of Stau1 on the interferon signature of the viral mimicry state. Using total RNA-seq, we confirmed that decitabine treatment resulted in a strong induction of many ISGs. We identified a total of 82 significantly up-regulated genes that were related to immune and response to virus (Fig. 4A, clusters 1 and 2). In addition, gene ontology (GO) analysis of the top 300 up-regulated genes using ClueGo and CluePedia revealed response to a type I interferon-related term (Fig. 4B). In addition to immune-related genes, decitabine treatment increased ribosome biogenesis (cluster 3), mitochondrial gene expression (cluster 4), mitotic cell cycle (cluster 5), and mitochondrial transport (cluster 6). Moreover, decitabine treatment also significantly decreased the expression of genes, which could be clustered to protein localization to the endoplasmic reticulum (cluster 7), mRNA splicing (cluster 8), and translation (cluster 9).

We then examined the effect of Stau1 knockdown on the genes that were significantly up- or down-regulated by decitabine. We found that most immune and virus-related genes in clusters 1 and 2 showed a significant decrease in the expression in Stau1-deficient cells (Fig. 4A). Indeed, the GO analysis on the top 500 down-regulated genes revealed response to type I interferon and other immune-related terms. This is consistent with our J2 dsRNA-seq analysis that Stau1 knockdown decreased ERV and Alu dsRNA expression levels and subsequently prevented the immune activation by decitabine. Interestingly, we

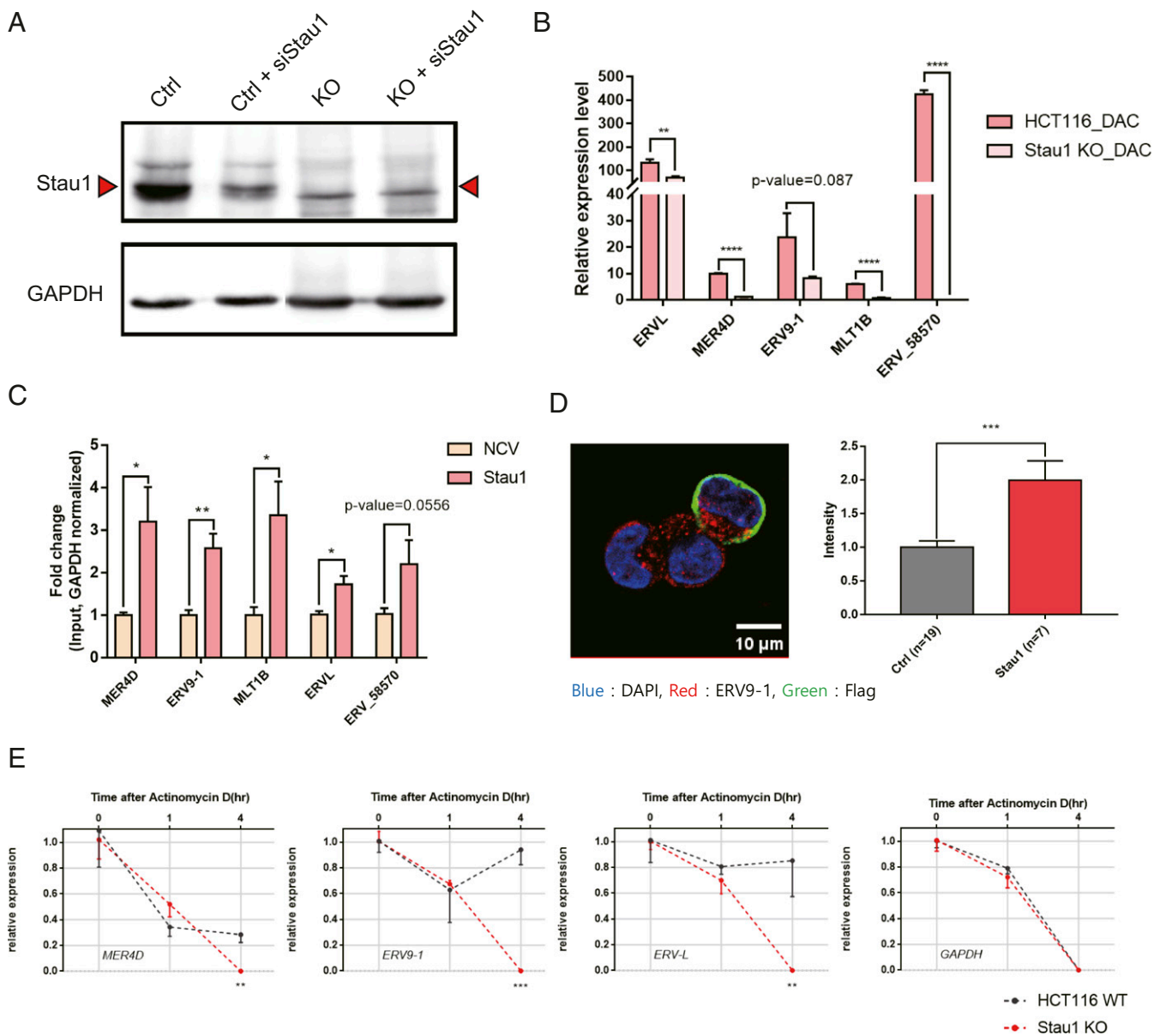


Fig. 3. Analysis of Stau1 KO cells reveals the stabilization of ERV RNAs by Stau1. (A) The Stau1 KO HCT116 cell is generated by targeting the exon 7 of Stau1 using CRISPR. Western blot analysis shows the elimination of the Stau1 band in the lysates from the KO cells. (B) Compared to the parental cells, Stau1 KO cells showed decreased levels of ERV RNAs when treated with decitabine. $n = 3$ and error bars denote SEM. (C) Overexpression of Stau1 in the KO cells resulted in increased expression of all ERVs examined. NCV indicates the transfection of the blank vector. (D) Increased expression of ERV9-1 RNA was also validated through RNA-FISH image analysis. Stau1-expressing cells were identified by staining cells with the Flag antibody, shown in green. Quantified fluorescent signals are shown on the *Right*. $n = 19$ (Ctrl), $n = 7$ (Stau1), and error bars denote SEM. (E) ERV RNA expression changes after treating parental and KO cells with ActD. $n = 3$ and error bars denote SEM. * P value < 0.05 , ** P value < 0.01 , *** P value < 0.001 , **** P value < 0.0001 .

found that other up-regulated genes in clusters 3 to 6 also showed decreased expression upon Stau1 knockdown. On the contrary, genes that were down-regulated by decitabine treatment were up-regulated in Stau1-deficient cells (Fig. 4A). Collectively, these data suggest that Stau1 knockdown virtually cancels the effect of decitabine not only in the induction of ISGs but also in other cell signaling systems.

We closely analyzed the ISGs that were regulated by decitabine and Stau1. The volcano plot analysis revealed that most of the highly affected genes by decitabine were ISGs, and that these ISGs showed significant down-regulation in Stau1-deficient cells (Fig. 4C). The fold change of the representative ISGs from the sequencing data are shown in Fig. 4D. Clearly, Stau1 knockdown eliminated the induction of ISGs by decitabine treatment. We further confirmed our

high-throughput sequencing data using RT-qPCR of the same group of ISGs, which showed a similar trend for nearly all of the genes tested (Fig. 4E). Lastly, we examined whether the expression of Stau1 itself was regulated by interferons. In our sequencing data, the expression of Stau1 did not change significantly. Moreover, we treated cells with interferon- β (IFN- β) and found that unlike ISGs, Stau1 expression was unchanged (Fig. 4F). Therefore, Stau1 and its stabilization of ERV RNAs are independent of IFN- β . Collectively, our data suggest that the Stau1 is critical in mediating the response to decitabine both in viral mimicry and others.

Patients with Low Stau1 Expression Show Inferior Response to the DNMTi Therapy. Although previous studies and the current study mainly used colorectal cancer cells, two DNMTis, azacitidine

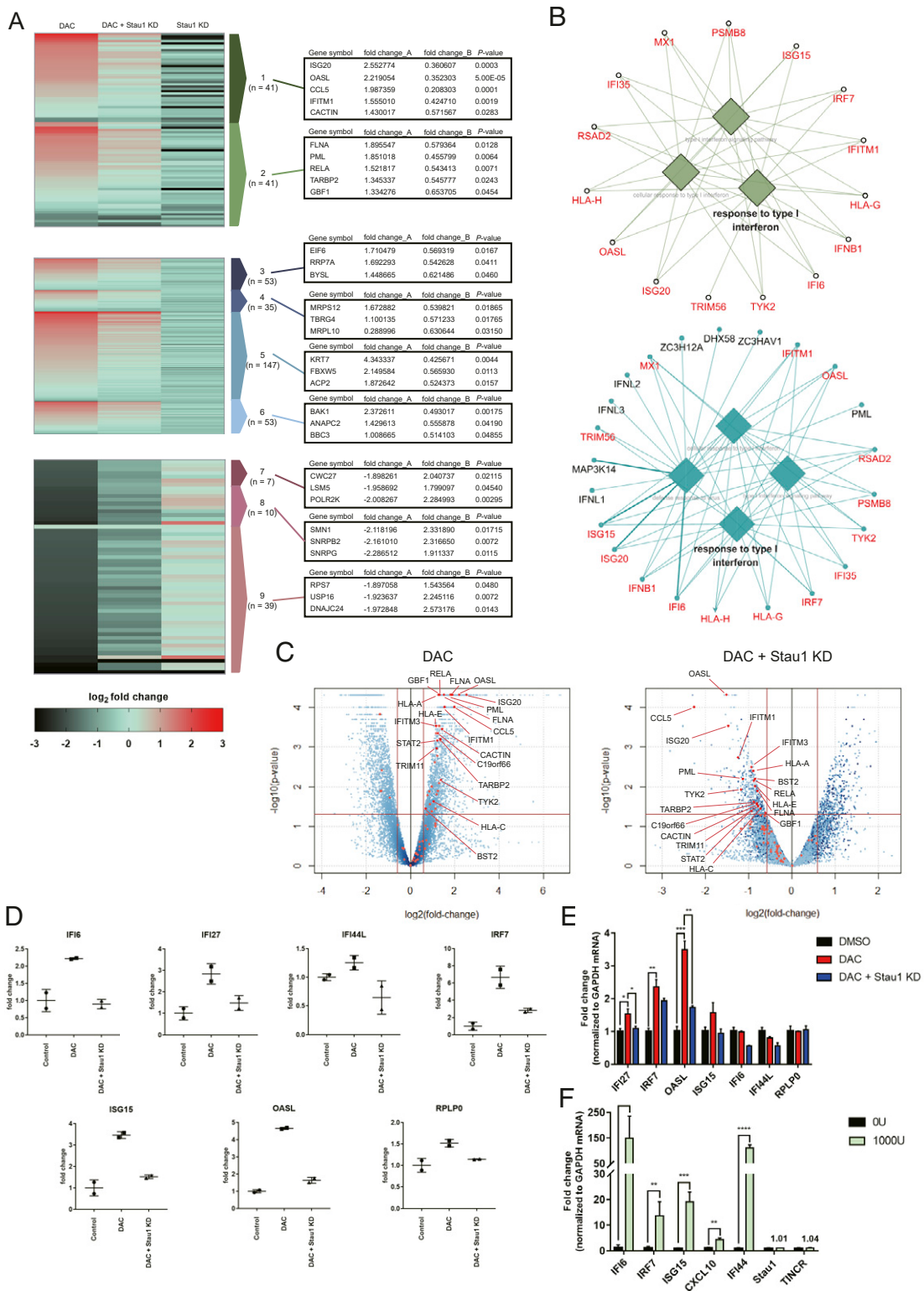


Fig. 4. Stau1 can regulate the immune response by decitabine. (A) Heatmap of total RNA sequencing results. The first column is the RNA expression ratio of siLuc+decitabine/siLuc+DMSO, the second column is the RNA expression ratio of siStau1+decitabine/siLuc+DMSO, and the third column is the RNA expression ratio of siStau1+DMSO/siLuc+DMSO. Fold_change_A indicates the expression change of the first column while fold_change_B denotes the expression change of the second column normalized by the first column (siStau1+decitabine/siLuc+decitabine). P values of the fold_change_B are shown in the third column. Cluster 1: related to immune, cluster 2: response to virus, cluster 3: ribosome biogenesis, cluster 4: mitochondrial gene expression, cluster 5: mitotic cell cycle, cluster 6: mitochondrial transport, cluster 7: protein localization to the endoplasmic reticulum, cluster 8: mRNA splicing, and cluster 9: translation. (B) GO of top 300 up-regulated genes after decitabine treatment (Top) and top 500 down-regulated genes in Stau1-deficient cells (Bottom). Overlapping genes are marked in red. (C) Volcano plot of the sequencing data with immune response-related genes indicated in red. The Left plot shows the RNA expression change by decitabine treatment, while the Right plot shows the RNA expression change in Stau1-deficient cells. (D) The RNA expression level of several ISGs in the total RNA-seq result. (E) Validation of the ISG expressions using RT-qPCR. n = 3 and error bars denote SEM. (F) Treating the cells with IFN-β did not affect the expression of Stau1 and TINCR. n = 3 and error bars denote SEM. *P value <0.05, **P value <0.01, ***P value <0.001, ****P value <0.0001.

and its deoxyderivative decitabine, have been approved to treat patients with MDS and AML. Thus, to investigate the clinical implications of our findings, we extended our analysis to MDS and AML. We first treated KG-1 acute myeloid leukemia cells with low-dose decitabine and confirmed the induction of numerous ERV RNAs (Fig. 5A). Interestingly, although most ERV RNAs showed increased expression, the identity of ERVs with the highest induction was different from that of HCT116 cells. Moreover, ERV9-1, which showed a strong induction in HCT116 cells, was down-regulated in KG-1 cells. This indicates that it is the combined level of total cellular dsRNAs rather than the expression of a single ERV element or a group of a few ERV elements that is necessary to induce the viral mimicry. Under this condition, we transfected cells with siStau1 and examined its effects. We found that the Stau1 knockdown significantly rescued cell death from decitabine in KG-1 cells by decreasing numerous ERV RNA expressions (Fig. 5B and C). This indicates that Stau1-mediated ERV stabilization is not limited to HCT116 cells, but may occur in other cell types as well.

We further extended our findings and analyzed samples of MDS and AML patients who underwent the DNMTi therapy. Between October 2015 and September 2018, 83 patients were diagnosed with MDS or AML and received either azacitidine or decitabine at the Seoul National University Hospital. Of these, 13 MDS patients were excluded after being found to be lower-risk MDS, and their goal of the DNMTi treatment was the correction of cytopenia rather than alternating the natural disease course. Other reasons for exclusion were: lack of or poor-quality bone marrow samples ($n = 18$) and nonevaluable to treatment response ($n = 6$; 3 due to early death before evaluation and 3 due to follow-up loss). In the end, 23 high-risk MDS and 23 AML patients were analyzed (SI Appendix, Table S1).

We extracted total RNAs from the bone marrow aspirates and analyzed the mRNA expression of several dsRBPs and ERV RNAs using RT-qPCR. When we examined the dsRBP mRNA expressions, we found that patients with poor response showed lower expression for most dsRBPs examined. Among these, only Stau1 showed a statistically significant difference between the two groups (Fig. 5D). When we dichotomize Stau1 expression into low (below median) versus high (equal or above median), low expression of Stau1 was associated with failure to achieve an objective response to DNMTis (SI Appendix, Table S2). Furthermore, low expression of Stau1 was associated with significantly inferior PFS and OS (Fig. 5E and F). Of note, when we examined the expression of ERV RNAs, we could not find any correlation with the patient responses (Fig. 5G). Considering that we analyzed the bone-marrow aspirates of patients before they received the DNMTi therapy, our results indicate that the basal ERV RNA levels do not have a diagnostic value in terms of predicting the responsiveness. At the same time, the basal expression of Stau1 prior to the therapy correlates with the therapy outcomes.

Stau1 Stabilizes ERV RNAs through Interaction with TINCR. Lastly, we sought out the mechanism through which Stau1 stabilized ERV RNAs. Although most previous studies focused on SMD (33), one study showed that Stau1 could stabilize differentiation-associated mRNAs when complexed with a long noncoding RNA TINCR (34). We asked whether TINCR also mediates the regulation of ERV RNAs through its interaction with Stau1. We found that TINCR RNA was expressed in HCT116 cells and was not regulated by either decitabine or IFN- β (Figs. 4F and 6A). In addition, TINCR strongly interacted with Stau1 (Fig. 6B). We then used RNAi to knockdown TINCR expression and analyzed its effect on ERV RNA levels. We found that in TINCR-deficient cells, many of the ERV RNAs under the regulation of decitabine were down-regulated (Fig. 6C and D and SI Appendix, Fig. S4A). Similarly, Alu RNAs were also down-regulated when we knocked down TINCR (SI Appendix, Fig. S4B). Of

note, when we analyzed ERV and Alu RNAs in Stau1 and TINCR double knocked down cells, we found an increased down-regulation for certain ERVs and AluSz_1976 (SI Appendix, Fig. S4A and B). This suggests that TINCR may also have Stau1-independent mechanisms to regulate the expression of ERV and Alu. We further performed Stau1 fCLIP and examined the interaction between Stau1 and ERV RNAs using RT-qPCR. We found that in TINCR-deficient cells, the interaction between Stau1 and ERV RNAs was significantly decreased (Fig. 6E). This indicates that TINCR enhances the binding between Stau1 and ERV RNAs, which may allow Stau1 to protect ERV RNAs from degradation.

Encouraged by these results, we further characterized the mode of interaction among ERV dsRNA, Stau1 protein, and TINCR RNA. First, we separated cytosolic and nucleic fractions and examined the ERV and TINCR RNA localization via RT-qPCR. We found that the nuclear-to-cytosolic expression ratios for all ERV RNAs analyzed and TINCR were less than 1, indicating these RNAs were cytosolic (SI Appendix, Fig. S5A). Moreover, through Western blotting, we also found that Stau1 was mostly expressed in the cytosol (SI Appendix, Fig. S5B). RNA-FISH of ERV9-1 and TINCR RNAs, together with immunocytochemistry of Stau1 protein, further confirmed the subcellular fractionation data (SI Appendix, Fig. S5C and D). Therefore, ERV, Stau1, and TINCR may form a complex in the cytosol.

Next, we examined the nature of this potential ternary complex. One possibility was that TINCR was first bound to ERV through sequence complementarity and the duplex was recognized by Stau1 for subsequent stabilization. Using the TINCR-binding motif identified by a previous study (34), we reanalyzed our J2 dsRNA-seq data and found that 25.44% of ERV loci that were up-regulated by decitabine contained at least one TINCR complementary site. Certain ERV elements such as LTR46-int even had 26 TINCR-binding motifs. Moreover, 26.08% of ERV loci that were down-regulated by Stau1 knockdown contained TINCR-binding motifs. This suggests that although certain types of ERVs may directly bind to TINCR, most Stau1-regulated ERVs do not.

If ERVs bind to Stau1 independently from TINCR, then the two must have noncompeting binding sites on the protein. To test, we generated a mutant Stau1 with two amino acid substitutions in its dsRBD 3 and 4, which impaired its ability to interact with dsRNAs (Fig. 6F) (35). We then expressed wild-type and mutant Stau1 and compared their ability to interact with ERV and TINCR RNAs. We found that while the mutant protein showed significantly decreased interaction with ERV RNAs, its interaction with TINCR was unaffected (Fig. 6G), indicating that Stau1-TINCR interaction occurs differently from that of Stau1-ERV. To map the TINCR-binding site, we expressed three different fragments of Stau1 protein (N terminal, dsRBD 3+4, and C terminal) and examined their relative interactions with ERV and TINCR RNAs (SI Appendix, Fig. S6A). We found that ERV RNAs were mostly bound to dsRBD 3+4 fragment while TINCR RNA showed stronger interaction with N- and C-terminal regions (SI Appendix, Fig. S6B and C). Combined, our data suggest that ERV and TINCR RNAs can bind to nonoverlapping regions on Stau1 protein to form a ternary complex in the cytosol.

Lastly, we investigated the clinical significance of TINCR expression by using the bone marrow aspirates from the 46 patients. Similar to that of Stau1, TINCR expression was lower in patients with poor response to DNMTis (Fig. 6H). Moreover, lower expression of Stau1 and TINCR was associated with significantly inferior PFS and OS compared to their counterparts (Fig. 6I and J). In multivariate analyses, Stau1^{low} TINCR^{low} was significantly associated with reduced PFS (hazard ratio [HR] 2.72, 95% CI 1.23 to 6.01; P value = 0.014) and OS (HR 4.97, 95% CI 1.73 to 14.27; P value = 0.003), respectively (SI Appendix, Tables S3 and S4). Stau1^{low} TINCR^{low} group also maintained the prognostic significance both in patients with or without complex karyotype in PFS and OS (SI Appendix, Fig. S7).

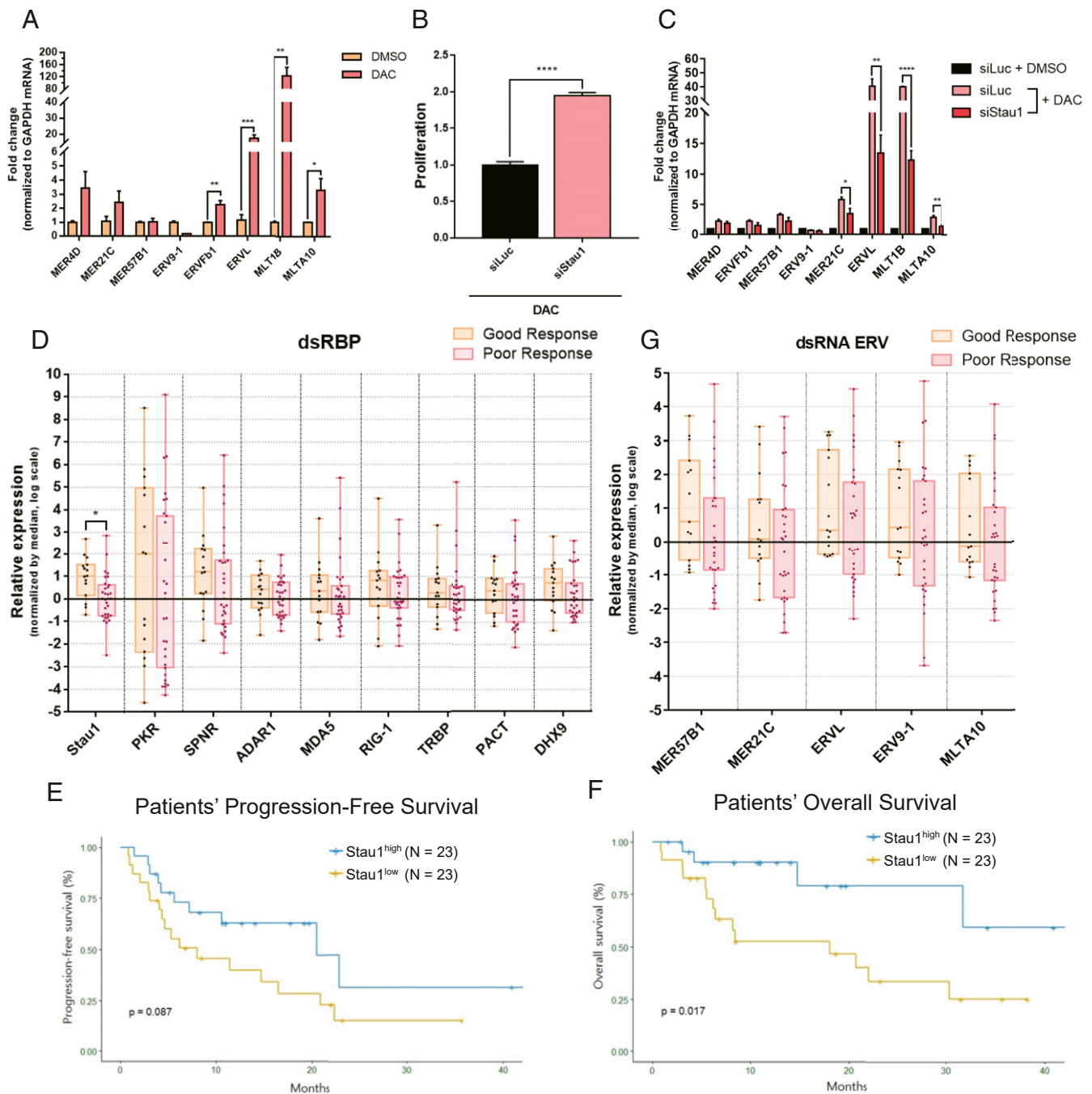


Fig. 5. MDS and AML patients with low Stau1 level show inferior response to the DNMTi therapy. (A) Transient low-dose exposure of decitabine resulted in the induction of several ERV RNAs in KG-1 AML cells. $n = 3$ and error bars denote SEM. (B) Knockdown of Stau1 significantly rescued the cell death from decitabine treatment in KG-1 cells. $n = 15$ and error bars denote SEM. (C) Stau1 knockdown also resulted in decreased expression of several ERV RNAs examined. $n = 3$ and error bars denote SEM. (D) Analysis of dsRBP mRNA expression from RNAs isolated from bone marrow aspirates from 46 MDS and AML patients. All patients received the DNMTi therapy, and samples were grouped based on the treatment outcome. (E and F) Patients with low Stau1 expression exhibited poor PFS (E) and OS (F) compared to those with high Stau1 mRNA expression. (G) Examining the basal expression of several ERVs in bone marrow aspirates of MDS and AML patients before receiving the DNMTi treatment. Patients are subcategorized into good or poor groups based on their response to the treatment. * P value <0.05 , ** P value <0.01 , *** P value <0.001 , **** P value <0.0001 .

Stau1-TINCR Mediates the Efficacy of Decitabine by Stabilizing ERV RNAs. Taken together, our study establishes Stau1 as a key regulatory factor required in the effective DNMTi therapy. In our model, the transcription of ERV RNAs is increased by exposure to decitabine. When transcribed, these RNAs are recognized by the Stau1-TINCR complex, which affects their subcellular localization and/or stability. The accumulation of stabilized ERV

RNAs can then trigger the downstream immune response mediated by PKR and MDA5, which induces interferons and transforms the cells into the viral mimicry state (Fig. 7).

Discussion

Our present data provide a noncanonical role of Stau1 in regulating the immune response to the DNMTi therapy by stabilizing

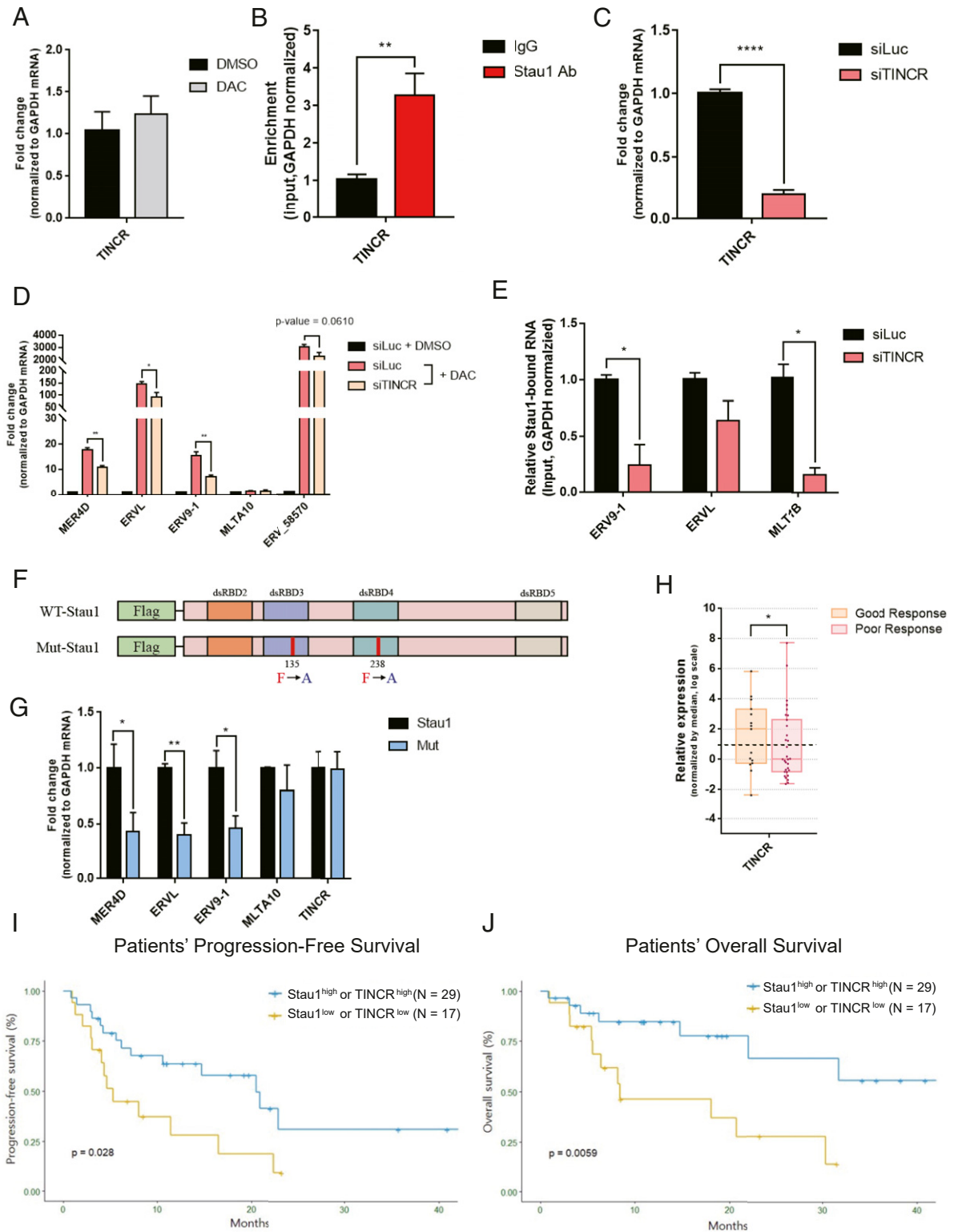


Fig. 6. TINCR noncoding RNA assists Stau1 in stabilizing ERV RNAs. (A) TINCR RNA expression in HCT116 cells was analyzed through RT-qPCR. $n = 3$ and error bars denote SEM. (B) Stau1 RNA-IP after formaldehyde cross-linking revealed that Stau1 strongly interacted with TINCR. $n = 3$ and error bars denote SEM. (C and D) Knockdown of TINCR using a siRNA resulted in decreased expression of TINCR (C) and ERV RNAs (D). $n = 3$ and error bars denote SEM. (E) In TINCR-deficient cells, the interaction between Stau1 and ERV RNAs was decreased. $n = 3$ and error bars denote SEM. (F) Schematic of wild-type and mutant Stau1 with impaired dsRNA binding. (G) dsRNA-binding mutant Stau1 showed significantly decreased interaction with ERV RNAs, but its interaction with TINCR was unaffected. (H) Analysis of TINCR RNA expression in 46 MDS/AML patient samples. Patients with poor response to the DNMTi therapy showed lower expression of TINCR. (I and J) Patients with low Stau1 and TINCR expressions exhibited inferior PFS (I) and OS (J) compared to those with high Stau1 or TINCR RNA expressions.

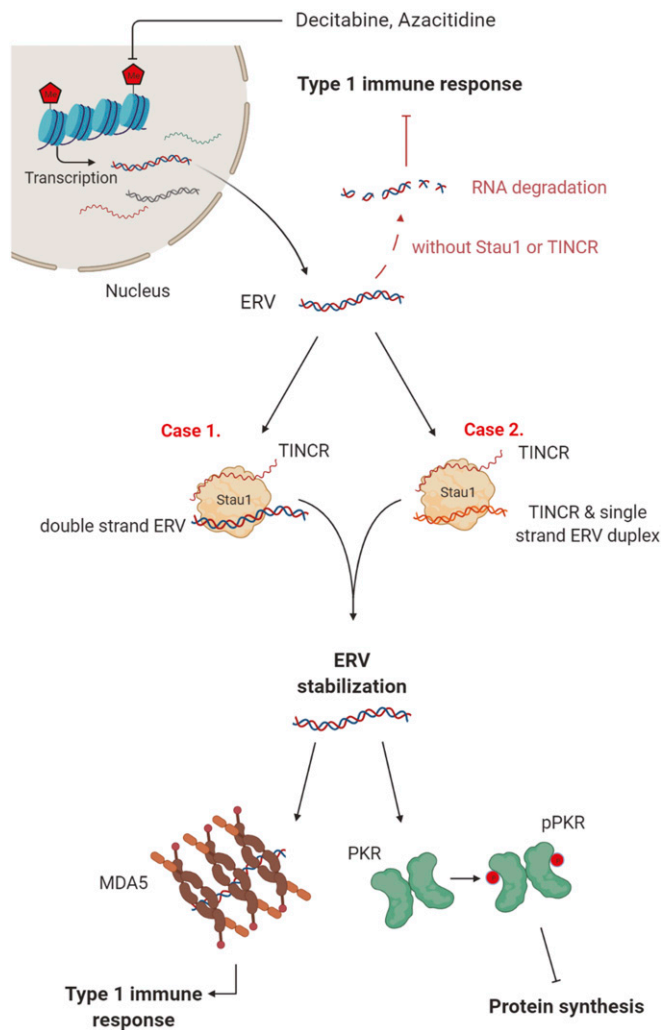


Fig. 7. Stau1 mediates the immune response by the DNMTi treatment by stabilizing ERV RNAs. Demethylation due to DNMTi treatment results in the induction of many cellular dsRNAs, including ERV RNAs. These RNAs are stabilized by Stau1 in complex with TINCR, which leads to the activation of dsRNA sensors of innate immune response proteins such as MDA5 and PKR. In the absence of Stau1 or TINCR, ERV RNAs are destabilized and fail to trigger an immune response, making the therapy ineffective. (Created with BioRender.com.)

ERV and Alu dsRNAs. Previous studies have established that DNMTi reduced the proliferation of cancer-initiating cells by activating dsRNA sensors of the innate immune system, transforming the cells into the viral mimicry state (19, 20). However, it remains unclear how these dsRNAs are being regulated at the posttranscriptional level. Remarkably, we found that the stability and/or subcellular localization of these immune triggering dsRNAs were under the regulation of Stau1 and TINCR. More importantly, AML and MDS patients with lower expression of Stau1 and TINCR showed significantly inferior response to the DNMTi therapy, suggesting that understanding the regulation of cellular dsRNAs by dsRBPs may provide the foundation for developing a patient-specific treatment strategy.

Both HCT116 and KG-1 cells showed good sensitivity to the transient low dose exposure to decitabine. In both cells, decitabine treatment resulted in strong induction of ERV RNAs and subsequent activation of viral defense response. Interestingly, the gene identity of ERVs that were regulated by decitabine was clearly different. ERV9-1 and ERVL were most strongly induced in HCT116 cells while in KG-1 cells, ERVL and MLT1B were

induced by more than 30-fold. These results also indicate that ERV RNAs responsive to the DNMTi treatment may differ from patient to patient. Indeed, previous clinical and fundamental studies could not pinpoint the ERV RNA that could be used as a response marker for the therapy. Considering that most dsRBPs, including the innate immune system, recognize the length of the target dsRNAs, the relevant marker might be the collective expression of all long dsRNAs. Recently, we developed an RNA intercalator-based sensor system that could detect total dsRNA expression in cells (36, 37). Indeed, the expression of total dsRNAs isolated from HCT116 cells treated with decitabine showed an increasing trend over time (36). Together with dsRBP expression, profiling the dynamic induction of total dsRNAs may provide valuable insights toward developing clinical biomarkers to predict the possible outcome of the DNMTi therapy.

Although many studies on DNMTi have been focused on ERVs, our J2 dsRNA-seq analysis clearly showed that other cellular dsRNAs were also involved. Notably, the fraction of ERV RNAs in our sequencing reads in the decitabine-treated sample was decreased compared to that of the control sample, despite the strong induction of ERV RNAs. This indicates that other cellular dsRNAs were also regulated, and most likely to a greater degree. We have previously shown that inverted Alu repeats occupy the largest fraction of PKR-activating cellular dsRNAs in human cells (22). In addition, LINE RNAs can also form double-stranded secondary structures that can activate PKR and trigger the immune response (22, 23). Our dsRNA-seq data and subsequent RT-qPCR data clearly show that Alu repeats are regulated by decitabine and Stau1. Consistent with our data, a recent study revealed that the major source of immunogenic dsRNAs induced by DNMTi is Alu (32). Therefore, applying the J2 antibody to examine the dsRNA expression profiles in various solid tumors and contexts may provide a better experimental approach in unraveling the molecular effects of the DNMTi treatment.

A key remaining question is how binding to Stau1 stabilizes ERV and Alu dsRNAs. One likely explanation is that Stau1 protects these dsRNAs from modifications that may mark the RNAs for decay. In addition, it is unclear how these Stau1-bound dsRNAs can be accessible by other dsRNA sensors, such as PKR and MDA5 to induce immune response. Clearly, our data suggest that Stau1 enhances the PKR activation and interferon response by dsRNAs. This contradicts a previous study where Stau1 and PKR compete for binding to Alu hairpin embedded in the 3' UTR of numerous mRNAs (13). However, we observed decreased interaction between PKR and ERV/Alu RNAs in Stau1-deficient cells. Perhaps, the noncoding dsRNAs may interact differently with Stau1 from hairpin stems in translating mRNAs. Alternatively, increased dsRNA expression beyond the physiological levels due to DNA demethylation may change how Stau1 and PKR interact with dsRNAs. The detailed molecular interaction between Stau1-dsRNA and with other dsRNA sensors should be investigated further in the future.

DNMTi have long been used to treat patients with MDS and AML. However, their exact mechanism of action has not been elucidated. They induce global hypomethylation of the genome, or so-called hypomethylating agents, but they restore only a part of aberrantly hypermethylated tumor suppressors (38). In fact, methylation status per se is not a marker for DNMTi's clinical benefit in MDS (39). Besides myeloid hematologic malignancies, DNMTi are receiving increasing attention to be used as a chemotherapy drug to treat solid tumors. Recent studies have shown that DNMTi and the subsequent immune response can potentiate sensitivity to immune checkpoint blockade and other immunotherapies (19, 20, 40). Under this background and trends, if the mechanism of action of DNMTi can be more explored from an immunological point of view and a reliable biomarker can be established, it can significantly improve the treatment outcomes of

patients with cancer. The identification of responsible dsRNAs and investigation on the posttranscriptional regulation of these dsRNAs would be a fair approach for the achievement. Although our study is focused on Stau1 and TINCR, our dsRBP screening data clearly reveal that multiple dsRBPs such as Stau1 and SPNR, may work together or work against each other such as in the case of Stau1 and PACT or DHX9. Moreover, other yet to be identified dsRBPs may also regulate the cellular response to DNMTis. Rigorous investigation on the dsRNA-dsRBP posttranscriptional regulatory network and the validation of the translational connotations through large clinical cohorts will greatly expand the applicability of DNMTis and cellular dsRNAs in fighting cancer.

Materials and Methods

Human Bone Marrow Aspirates. To investigate whether pretreatment dsRBP expression is associated with treatment outcomes in patients with newly diagnosed higher-risk MDS (HR-MDS; intermediate-2 or high-risk group according to the International Prognostic Scoring System [IPSS]) (41) or AML and received DNMTis as the frontline therapy, RNAs were extracted from the patients' bone marrow aspirates that were cryopreserved with RNAlater stabilizer before initiation of the DNMTi treatment. Subsequently, RNAs were purified using the Nucleospin RNA/Protein kit (Macherey-Nagel) following the manufacturer's instructions. All patients were diagnosed either HR-MDS or AML according to the World Health Organization classification criteria for myeloid neoplasms (42) and received either azacitidine or decitabine. Patients who were diagnosed with lower-risk MDS or myeloid malignancies other than MDS or AML, who lacked clinical information or bone marrow samples, and who were not evaluable for response to DNMTis, were excluded from the analysis. The use of clinical data and the secondary use of preserved samples from the biorepository with all patients' informed consent were reviewed and approved by the Institutional Review Board (IRB) of

Seoul National University Hospital, Seoul, Republic of Korea (IRB no. H-1810-002-974).

RNA-FISH. For RNA-FISH, cells were seeded on an eight-well slide and incubated for 1 d. Cells were rinsed once with phosphate-buffered saline (PBS) and fixed in 4% wt/vol paraformaldehyde (PFA) for 10 min at room temperature. Cells were rinsed 2 times in PBS and washed once in PBS for 5 min. To permeabilize the cells, cells were kept in 70% ethanol in 2× saline sodium citrate (SSC) overnight in 4 °C. Cells were rehydrated by a successive wash in 50% ethanol and 25% ethanol for ~2 to 3 min each. Cells were then washed two times in 2× SSC for 10 min each and incubated 50% formamide for 2 h at 40 °C. Cells were hybridized with denatured probes for 4 h at 40 °C. Cells were washed two times in 2× SSC in 50% formamide at 37 °C and two times in 0.1× SSC in 50% formamide at 37 °C for 30 min each. Cells were then blocked in 0.2% bovine serum albumin (BSA), 8% formamide, 2× SSC for 1 h. Sheep anti-DIG (Sigma-Aldrich) was used as the primary antibody, and fluorophore-labeled secondary antibody was used to visualize the RNAs. Cells were imaged with a Carl Zeiss LSM 780 confocal microscope with a 63× objective (NA = 1.40). Images were analyzed with ImageJ software.

Data Availability. The high-throughput sequencing data reported in this paper is available at the National Center for Biotechnology Information (NCBI) Gene Expression Omnibus database, accession [GSE152258](https://www.ncbi.nlm.nih.gov/geo/query/acc.cgi?acc=GSE152258).

ACKNOWLEDGMENTS. We thank the members of our laboratories for their input and helpful discussions. We also thank S. C. Kwon and V. N. Kim (Seoul National University) for their advice about generating CRISPR KO cells. This research was supported by the Korean government Ministry of Science and ICT (NRF-2019R1C1C1006672 to Y. Kim) (NRF-2013M3A9B5076486 to D.S.) and the KAIST Future Systems Healthcare Project (KAISTHEALTHCARE42 to Y. Kim).

- Schlee, G. Hartmann, Discriminating self from non-self in nucleic acid sensing. *Nat. Rev. Immunol.* **16**, 566–580 (2016).
- Pettersson, L. Philipson, Synthesis of complementary RNA sequences during productive adenovirus infection. *Proc. Natl. Acad. Sci. U.S.A.* **71**, 4887–4891 (1974).
- Weber, V. Wagner, S. B. Rasmussen, R. Hartmann, S. R. Paludan, Double-stranded RNA is produced by positive-strand RNA viruses and DNA viruses but not in detectable amounts by negative-strand RNA viruses. *J. Virol.* **80**, 5059–5064 (2006).
- Hur, Double-stranded RNA sensors and modulators in innate immunity. *Annu. Rev. Immunol.* **37**, 349–375 (2019).
- Akira, S. Uematsu, O. Takeuchi, Pathogen recognition and innate immunity. *Cell* **124**, 783–801 (2006).
- Kostura, M. B. Mathews, Purification and activation of the double-stranded RNA-dependent eIF-2 kinase DAI. *Mol. Cell. Biol.* **9**, 1576–1586 (1989).
- Thomis, C. E. Samuel, Mechanism of interferon action: Evidence for intermolecular autophosphorylation and autoactivation of the interferon-induced, RNA-dependent protein kinase PKR. *J. Virol.* **67**, 7695–7700 (1993).
- Lemaire, E. Anderson, J. Lary, J. L. Cole, Mechanism of PKR activation by dsRNA. *J. Mol. Biol.* **381**, 351–360 (2008).
- Wek, H. Y. Jiang, T. G. Anthony, Coping with stress: eIF2 kinases and translational control. *Biochem. Soc. Trans.* **34**, 7–11 (2006).
- Lander et al.; International Human Genome Sequencing Consortium, Initial sequencing and analysis of the human genome. *Nature* **409**, 860–921 (2001).
- Athanasias, A. Rich, S. Maas, Widespread A-to-I RNA editing of Alu-containing mRNAs in the human transcriptome. *PLoS Biol.* **2**, e391 (2004).
- Liu et al., Structure and degradation of circular RNAs regulate PKR activation in innate immunity. *Cell* **177**, 865–880.e21 (2019).
- Elbarbary, W. Li, B. Tian, L. E. Maquat, STAU1 binding 3' UTR IRALus complements nuclear retention to protect cells from PKR-mediated translational shutdown. *Genes Dev.* **27**, 1495–1510 (2013).
- Ahmad et al., Breaching self-tolerance to Alu duplex RNA underlies MDA5-mediated inflammation. *Cell* **172**, 797–810.e13 (2018).
- Liddicoat et al., RNA editing by ADAR1 prevents MDA5 sensing of endogenous dsRNA as nonself. *Science* **349**, 1115–1120 (2015).
- Chen, G. G. Carmichael, Gene regulation by SINES and inosines: Biological consequences of A-to-I editing of Alu element inverted repeats. *Cell Cycle* **7**, 3294–3301 (2008).
- Kim et al., PKR is activated by cellular dsRNAs during mitosis and acts as a mitotic regulator. *Genes Dev.* **28**, 1310–1322 (2014).
- Bahn et al., Genomic analysis of ADAR1 binding and its involvement in multiple RNA processing pathways. *Nat. Commun.* **6**, 6355 (2015).
- Chiappinelli et al., Inhibiting DNA methylation causes an interferon response in cancer via dsRNA including endogenous retroviruses. *Cell* **162**, 974–986 (2015).
- Roulois et al., DNA-demethylating agents target colorectal cancer cells by inducing viral mimicry by endogenous transcripts. *Cell* **162**, 961–973 (2015).
- Dhir et al., Mitochondrial double-stranded RNA triggers antiviral signalling in humans. *Nature* **560**, 238–242 (2018).
- Kim et al., PKR senses nuclear and mitochondrial signals by interacting with endogenous double-stranded RNAs. *Mol. Cell* **71**, 1051–1063.e6 (2018).
- Kim, Y. Ku, J. Ku, Y. Kim, Evidence of aberrant immune response by endogenous double-stranded RNAs: Attack from within. *BioEssays* **41**, e1900023 (2019).
- Rice et al., Mutations in ADAR1 cause Aicardi-Goutières syndrome associated with a type I interferon signature. *Nat. Genet.* **44**, 1243–1248 (2012).
- Banerjee et al., OAS-RNase L innate immune pathway mediates the cytotoxicity of a DNA-demethylating drug. *Proc. Natl. Acad. Sci. U.S.A.* **116**, 5071–5076 (2019).
- Liu et al., Vitamin C increases viral mimicry induced by 5-aza-2'-deoxycytidine. *Proc. Natl. Acad. Sci. U.S.A.* **113**, 10238–10244 (2016).
- Patel, P. Stanton, N. M. McMillan, B. R. Williams, G. C. Sen, The interferon-inducible double-stranded RNA-activated protein kinase self-associates in vitro and in vivo. *Proc. Natl. Acad. Sci. U.S.A.* **92**, 8283–8287 (1995).
- Saunders, G. N. Barber, The dsRNA binding protein family: Critical roles, diverse cellular functions. *FASEB J.* **17**, 961–983 (2003).
- Ricci et al., Stau1 senses overall transcript secondary structure to regulate translation. *Nat. Struct. Mol. Biol.* **21**, 26–35 (2014).
- Aktaş et al., DHX9 suppresses RNA processing defects originating from the Alu invasion of the human genome. *Nature* **544**, 115–119 (2017).
- Gong, L. E. Maquat, lncRNAs transactivate STAU1-mediated mRNA decay by duplexing with 3' UTRs via Alu elements. *Nature* **470**, 284–288 (2011).
- Mehdipour et al., Epigenetic therapy induces transcription of inverted SINEs and ADAR1 dependency. *Nature* **588**, 169–173 (2020).
- Park, L. E. Maquat, Stau1-mediated mRNA decay. *Wiley Interdiscip. Rev. RNA* **4**, 423–435 (2013).
- Kretz et al., Control of somatic tissue differentiation by the long non-coding RNA TINCR. *Nature* **493**, 231–235 (2013).
- Luo, T. F. Duchaine, L. DesGroseillers, Molecular mapping of the determinants involved in human Stau1-ribosome association. *Biochem. J.* **365**, 817–824 (2002).
- Ali, M. Kang, R. Kharbush, Y. Kim, Spiropyran as a potential molecular diagnostic tool for double-stranded RNA detection. *BMC Biomed. Eng.* **1**, 6 (2019).
- Ali, R. Kharbush, Y. Kim, Chemo- and biosensing applications of spiropyran and its derivatives—A review. *Anal. Chim. Acta* **1110**, 199–223 (2020).
- Sato, J. J. Issa, P. Kropf, DNA hypomethylating drugs in cancer therapy. *Cold Spring Harb. Perspect. Med.* **7**, a026948 (2017).
- Voso et al., Why methylation is not a marker predictive of response to hypomethylating agents. *Haematologica* **99**, 613–619 (2014).
- Wang, Y. Liu, Y. Cheng, Y. Wei, X. Wei, Immune checkpoint blockade and its combination therapy with small-molecule inhibitors for cancer treatment. *Biochim. Biophys. Acta Rev. Cancer* **1871**, 199–224 (2019).
- Greenberg et al., International scoring system for evaluating prognosis in myelodysplastic syndromes. *Blood* **89**, 2079–2088 (1997).
- Arber et al., The 2016 revision to the World Health Organization classification of myeloid neoplasms and acute leukemia. *Blood* **127**, 2391–2405 (2016).